

## CHARACTERIZATION OF UNSTABLE POINT DEFECTS IN CRYSTALS

I.V. Ostrovskii and O.A. Korotchenkov

Faculty of Physics, Kiev State University, Kiev, 252022, Ukraine

(Received 26 September 1991 by J. Joffrin; revised 12 December 1991)

Investigation of unstable defects generated by ultra-sound in ZnS and ZnSe crystals is reported. The experimental techniques use simultaneously both optical and acoustic excitation of crystal. Acousto-photoconductivity (APC) and acoustophotoluminescence (APL) were measured under the above-threshold intensity of ultrasound. By these measurements both deep and shallow energy levels of point defects and their complexes can be found.

### 1. INTRODUCTION

THE PROBLEM of crystal defects (point and linear) is of great interest for many reasons. There is a number of methods for studying defects and their related-energy levels in the band gap [1–5]. It is now commonplace to use laser spectroscopy, EPR and ODMR techniques, DLTS, etc. Optical and EPR studies coupled with uniaxial stress could also be a useful method for point defects investigation. Normally the stable defects are studied. The configuration of these defects in the lattice is constant at a given temperature. However, there is an interesting problem of unstable defects characterization, for example the donor-acceptor pairs with the small distance ( $r_{AD}$ ) between them. The point is that the pairs with  $r_{AD}$  equal to some lattice periods possess a small life time and annihilation begins at 60 K [6]. The most important example of such kind of defects is radiation damage ones.

The method proposed allows us to characterize both unstable and stable defects. The physical basis for this method consists in defects generation by acoustic wave (AW). The unstable defects can be characterized by studying some crystal properties (spectra) during ultrasonic action on the sample. To our knowledge, no reports have been published of unstable defects characterization at room temperature.

### 2. EXPERIMENTAL DETAILS

Single crystals of ZnS, ZnS: Ag and ZnSe (used in lasers) with the sphalerite and wurtzite structure have been experimentally investigated at room temperature. The concentration of Ag impurities was  $10^{-4}$  and  $10^{-2}$  at %. Samples with the next dimensions: length 5–12 mm, cross-section from  $2 \times 2$  to  $5 \times 5$  mm<sup>2</sup> were cleaved from a massive boule. Piezoelectric ceramic transducers were bounded to the

opposite faces of the sample and excited a longitudinal acoustic wave in this sample. The frequency of AW was constant (2 MHz). Photoconductivity investigation was carried out by photoresistance measurements between ohmic In–Ga contacts. The conductivity was determined at right-angles to the wave vector of AW in order to avoid the influence of possible longitudinal acoustoelectric effect. The region between the contacts was illuminated via a monochromator with modulated or constant light from a high-power (500 W) source. A pulse nitrogen laser excited the photoluminescence of the sample. A 0.343 m double monochromator dispersed the luminescence which was detected by a photomultiplier tube.

### 3. RESULTS AND DISCUSSIONS

#### 3.1. Deep-level defects

The unstable point defects are characterized by photoconductivity spectra measurements in the presence of AW (APC-method). In Fig. 1 spectra of ZnS crystal are shown. The spectrum 1 is obtained in the absence of AW in the sample. The weak PC band in the region of 2.8 eV corresponds to the sulfur vacancies  $V_s^+$  [7]. Injection of low-intensity AW into the sample does not essentially modify the PC spectrum, but further increase in the AW intensity (W) changes it considerably (spectra 2, 3). There is an increase in the photoconductivity over the whole spectrum. In addition, a new bands appear at 3.25 and 3.52 eV. Finally, the band near 2.80 eV becomes stronger. These considerable changes completely disappear after the AW removal.

Analysing the results obtained one should account for the threshold nature of the AW action. The threshold intensity  $W_{th}$  range from 0.5 to 1.0 W cm<sup>-2</sup> for the different ZnS samples and is equal to 1.5 W cm<sup>-2</sup> for

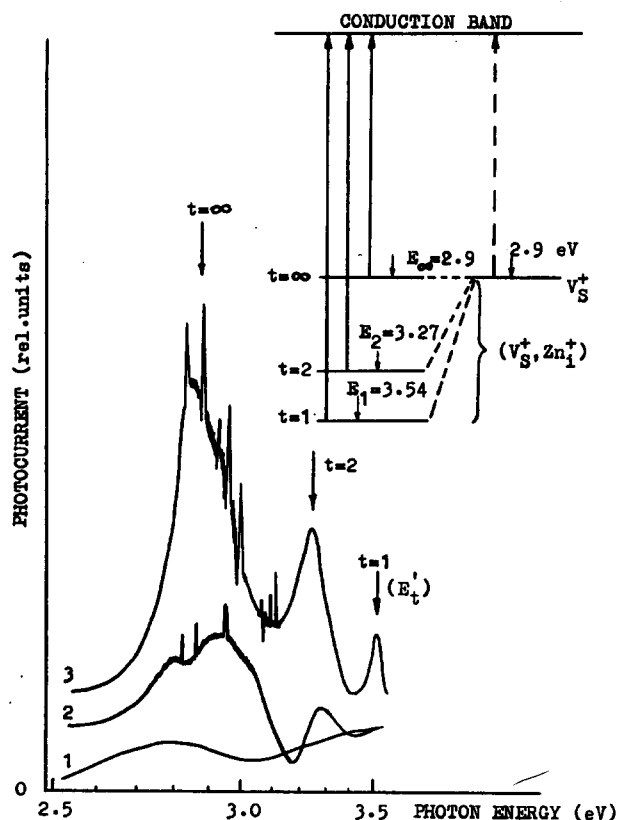


Fig. 1. The complex  $(V_s^+, Zn_i^+)$  characterization in ZnS:  $10^{-4}\%$  Ag sphalerite sample by APC spectra investigation. 1 without AW; 2  $W = W_{th} \approx 0.5 \text{ W cm}^{-2}$ ; 3  $W = 1.7 W_{th}$ . The energies  $E_i$  and  $E'_i$  are calculated from equations (1) and (5) for  $r_i = 2.70 \text{ \AA}$  ( $t = 1$ ),  $4.68$  ( $t = 2$ ),  $\infty$  ( $t = \infty$ ). The dashed arrow on the diagram corresponds to the APC spectrum without ultrasound.

ZnSe. This value corresponds to the beginning of structural defects generation by AW [8]. Differences obtained in  $W_{th}$  value is caused by different concentrations of the dislocations and their obstacles in the sample. The threshold is associated with unpinning of dislocations from the obstacles and with the onset of their vibrational motion in the deformation field created by acoustic wave. The defects generated is unstable, mobile and located at different distances from one another, so that one could expect all possible atomic configurations of point defects and their complexes in a given sample. Life time measurements of unstable donor-acceptor pairs in CdS show the value less than  $10^{-5} \text{ s}$ . The results presented in Fig. 1 make it possible to characterize a group of  $(V_s^+, Zn_i^+)$  levels. These levels are shown in the inset in Fig. 1 and correspond to  $V_s^+$  in a Coulomb field of the ion  $Zn_i^+$  (donor, interstitial zinc), calculated from the following

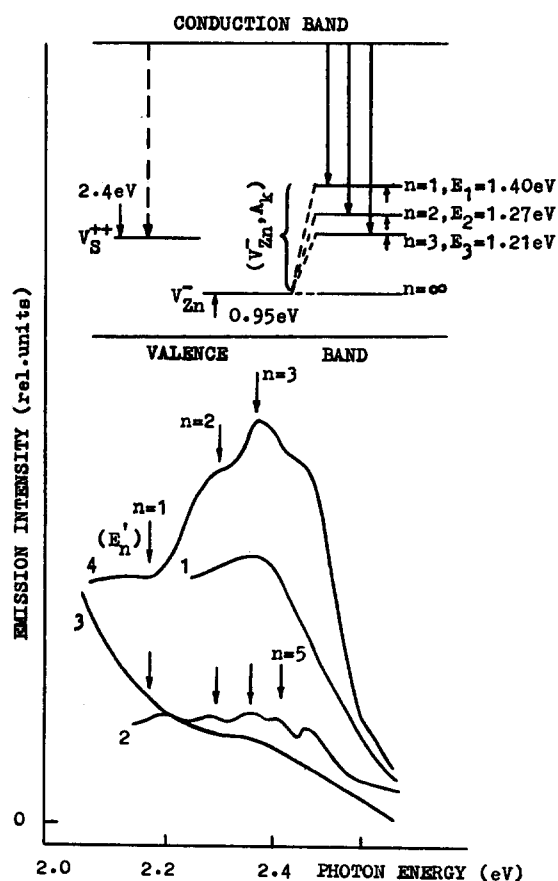


Fig. 2. The complex  $(V_{Zn}^-, A_k)$  characterization in ZnS (1, 2) and ZnS:  $10^{-2}\%$  Ag (3, 4) sphalerite samples by APL spectra investigation. 1, 3 without AW; 2, 4  $W = 1.2 W_{th} \approx 1.0$  (spectrum 2) and  $0.8$  (4)  $\text{W cm}^{-2}$ . The energies  $E_n$  and  $E'_n$  are calculated from equations (2) and (6) for  $r_n = 3.83 \text{ \AA}$  ( $n = 1$ ),  $5.41$  ( $n = 2$ ),  $6.63$  ( $n = 3$ ),  $8.56$  ( $n = 5$ ). The dashed arrow on the diagram corresponds to the PL spectrum without AW.

equation:

$$E_i = E_{V_s^+} + q^2/\epsilon r_i, \quad (1)$$

where  $E_{V_s^+}$  and  $E_i$  are the energies of the vacancy  $V_s^+$  and of the complex  $(V_s^+, Zn_i^+)$ ,  $r_i$  is the distance between the  $V_s^+$  and  $Zn_i^+$ . Comparison of the calculated  $E_i$  levels with the bands of APC spectra shows a good agreement.

For illustrative purposes we have also investigated the photoluminescence spectra under AW action (APL-method). An acoustic wave with above-threshold intensity produces bands in the PL spectra being absent in the specimens which are not loaded by ultrasound. The results both for ZnS and ZnS: Ag samples are shown in Fig. 2. We can conclude that the APL bands observed must be attributed to the system of

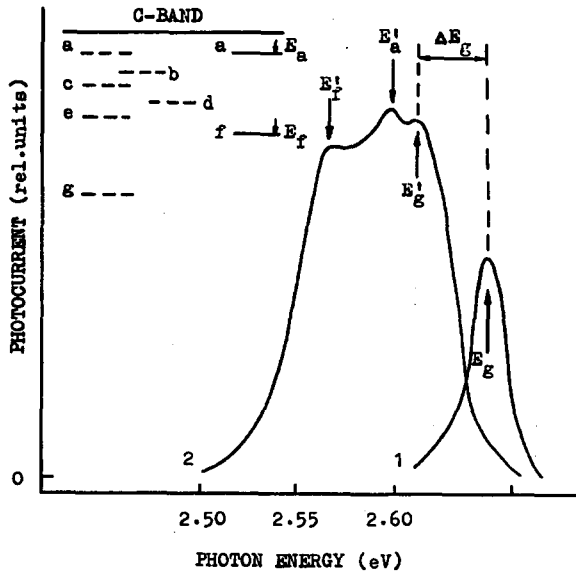


Fig. 3. Characterization of the shallow donors in ZnSe sphalerite sample by APC spectra. 1 without AW; 2  $W = 1.2 W_{th}$ . The value of  $W_{th} \approx 1.5 W cm^{-2}$ . Energies  $E_d$  of donor levels are shown schematically (meV): (a) 10 [11]; (b) 15 [12]; (c) 21 [13]; (d) 28 [14]; (e) 34 [15]; (f) 40; (g) 70 [16, 17].

deep donor levels  $V_{Zn}^-$  (zinc vacancy) in the Coulomb field of a singly charged acceptor  $A_k$  located at a cation site (for example, Ag impurity). These levels are shown in the inset in Fig. 2 and were calculated as

$$E_n = E_{V_{Zn}^-} + q^2/\epsilon r_n. \quad (2)$$

The  $(V_{Zn}^-, A_k)$  complex concentration is considerably increased by Ag doping. The consequence is that AW action increases PL intensity in ZnS:Ag samples (spectra 4 in Fig. 2) and decreases it in ZnS (spectra 2). Finally it should be noted that APL band at 2.48 eV (spectra 2 and 4 in Fig. 2) and photocurrent fluctuation at APC spectra in the region of 2.8–3.0 eV (2 and 3 in Fig. 1) are related to the energy levels of moving dislocations. We shall discuss this problem elsewhere.

### 3.2. Shallow-level defects

Acoustic wave of above-threshold intensity also generates different donor centers, acceptor centers and complexes of point defects with different energy levels close to the bottom of conduction band and top of valence band. Mainly these states are ionized, and, thus, APC-spectrum can be measured to determine energy levels of shallow defects. Figure 3 shows the intrinsic photoconductivity of ZnSe with the maximum at 2.64 eV (arrow  $E_g$  at spectrum 1). Excitation of AW in the sample shifts this band toward lower energies (arrow  $E'_g$  at spectrum 2 in Fig. 3). Similar

effect is observed in ZnS samples. The shift increases with the increasing of the ultrasound intensity. This shift reaches its maximum value of 40–45 meV, which corresponds to reduction in the band gap  $E_g$  of the crystal investigated under the influence of AW. Reduction in  $E_g$  can be represented by

$$\Delta E_g = \Delta E_T + \Delta E_A + \Delta E_p + \Delta E_d + \Delta E_i, \quad (3)$$

where the remaining terms represent contributions of sample heating under AW action ( $\Delta E_T$ ), acoustic deformation ( $\Delta E_A$ ), piezoelectric field associated with AW ( $\Delta E_p$ ), electric fields of charged dislocations ( $\Delta E_d$ ), and of point defects generated by AW ( $\Delta E_i$ ). To estimate quantitatively the contributions of these terms special experimental study and theoretical calculations of ultrasonic influence on light transmission spectra have been carried out. The samples were treated by temperature and external electric field. Results obtained were compared with the theoretical calculations, including electrical fields of point defects and dislocations [9]. Experimentally  $\Delta E_g$  can be found as the difference:

$$\Delta E_g = E_g - E'_g. \quad (4)$$

This shift is used for proper calculations of the energies of electronic transitions which are presented in Fig. 1 (spectrum 3) and Fig. 2 (spectra 2, 4) by the arrows. These energies, i.e.:  $E'_i$  (Fig. 1) and  $E'_n$  (Fig. 2) are calculated as the following differences:

$$E'_i = E_i - \Delta E_g, \quad (5)$$

$$E'_n = E_n - E_n - \Delta E_g. \quad (6)$$

When the  $W_{th}$  intensity is reached, the APC spectra of ZnSe and ZnS broadens and new bands appear (2 in Fig. 3, 2 and 4 in Fig. 4). These changes confirm the appearance of shallow donor centers and their complexes under AW action. These centers are ionized both thermally ( $kT \approx 0.026$  eV at room temperature) and by AW. Ionization of local states by ultrasound was experimentally confirmed in [10], the physical nature of this effect is due to vibration of charged dislocation in ultrasonic field of acoustic wave with the above-threshold intensity. Therefore, the centers appeared manifest themselves in the long-wavelength edge of the APC band. The energy positions of the maxima in the spectra 2 (Fig. 3) and 2, 4 (Fig. 4) were used to estimate the depth of the donors generated by AW. For example:

$$E_a = E'_g - E'_a, \quad E_f = E'_g - E'_f. \quad (7)$$

The energy schemes in Figs. 3 and 4 show energy levels estimated (continuous lines) and the published data [11–19] (dashed lines). This introduction of AW creates intrinsic defects, and one can assume that the donor

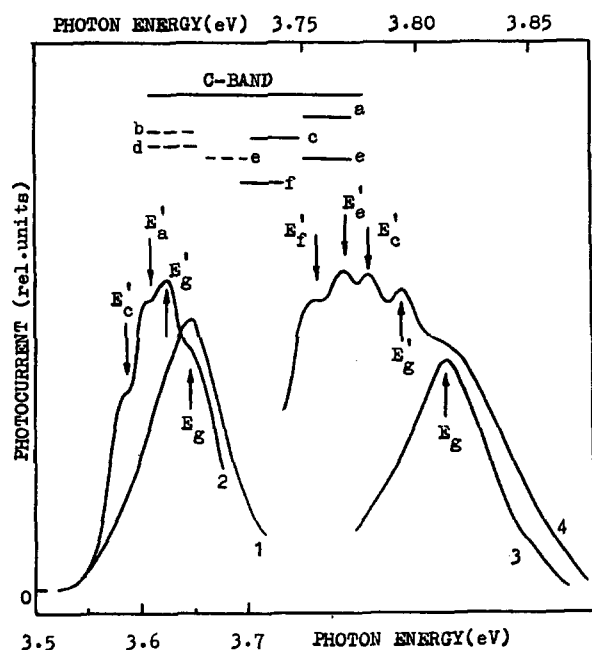


Fig. 4. Characterization of the shallow donors in ZnS sphalerite (1, 2) and wurtzite (3, 4) samples by APC spectra. 1, 3 without AW; 2  $W = 1.7 W_{th}$ ; 4  $W = 2.6 W_{th}$ . The value of  $W_{th} \approx 1.3$  (spectrum 2) and 1.0 (4)  $W_{cm}^{-2}$ . Depth of donor levels  $E_d$  (meV): (a) 11; (b) 18 [18]; (c) 20; (d) 22.5 [18]; (e) 30 [19]; (f) 40.

states with the depths of 10 and 40 meV in ZnSe and 11, 20, 30 and 40 meV in ZnS are due to intrinsic point defects and their complexes. The remaining levels shown in the energy schemes in Figs. 3 and 4 are clearly due to impurity centers.

It should be mentioned that further AW intensity increasing gives rise to the intensity of the line (f) with some of ZnSe samples and it is accompanied by a simultaneous suppression of line (a) (spectra 2 in Fig. 3). This phenomenon can be tentatively attributed to the formation of large clusters of point defects under the influence of high-intensity AW. The characteristic rise time of this PC line and its disappearance after AW removal range from 20 to 90 s.

#### 4. CONCLUSIONS

The basic results of the present experiments can be summarized as follows:

(1) The unstable point defects are investigated by the new experimental technique, which simultaneously uses ultrasound and light excitation of the sample.

(2) For shallow level defects characterization it is necessary to measure APC spectra near the absorption edge energy. APC and APL spectra with the photon energy less than forbidden band width have to be measured for deep level defects characterization.

(3) The above mentioned method application results in discovery of shallow donor states with depths of 10 and 40 meV below the bottom of the conduction band in ZnSe crystals and of 11, 20, 30 and 40 meV in ZnS. These states are due to intrinsic point defects and their complexes. We have also observed the deep level ( $V_i^+$ ,  $Zn_i^+$ ) and ( $V_{Zn}^-$ ,  $A_k$ ) complexes in ZnS crystals.

#### REFERENCES

1. B.H. Bairamov, G. Irmer, J. Monecke & V.V. Toropov, *J. Molec. Struct.* **219**, 19 (1990).
2. I. Minoru, *Bull. Jap. Inst. Metals* **29**, 191 (1990).
3. K.M. Lee, Le Di Dang & G.D. Watkins, *Solid State Commun.* **35**, 527 (1980).
4. D.V. Lang, *J. Appl. Phys.* **45**, 3023 (1974).
5. K. Dmowski, *Rev. Sci. Instrum.* **61**, 1319 (1990).
6. G.D. Watkins, *Radiation Effects in Semiconductors*, The Institute of Physics, Bristol and London (1977).
7. P. Pecheur, E. Kauffer & M. Gerl, *Inst. Phys. Conf. Ser.* **31**, 458 (1977); J. Schneider & A. Rauber, *Solid State Commun.* **5**, 779 (1967).
8. I.V. Ostrovskii, *JETP Lett.* **34**, 446 (1981); I.V. Ostrovskii & V.N. Lysenko, *Sov. Phys. Solid State* **24**, 682 (1982).
9. I.V. Ostrovskii & O.A. Korotchenkov, *Ukrainian Phys. J.* **30**, 356 (1985).
10. I.V. Ostrovskii, A.Kh. Rozhko & V.N. Lysenko, *Sov. Phys. Solid State* **23**, 907 (1981).
11. H. Roppischer, J. Jacobs & V.B. Novikov, *Phys. Status Solidi (a)* **27**, 123 (1975).
12. P.J. Dean & I.H. Jones, *Phys. Rev.* **A133**, 1698 (1964).
13. V. Swaminathan & L.C. Greene, *Phys. Rev.* **B14**, 5351 (1976).
14. T. Taguchi & B. Ray, *Progr. Crystal Growth and Charact.* **6**, 103 (1983).
15. P.J. Dean & J.L. Merz, *Phys. Rev.* **178**, 1310 (1969).
16. J.L. Merz, K. Nassau & J.W. Shiever, *Phys. Rev.* **B8**, 1444 (1973).
17. D. Etienne, J. Ellegre, J. Chevrier & G. Bougnot, *Phys. Status Solidi (a)* **32**, 279 (1975).
18. M.A.S. Sweet & D. Urquhart, *Phys. Status Solidi (a)* **59**, 223 (1980).
19. Yu. V. Voronov, *Tr. Fiz. Inst. Akad. Nauk SSSR* **68**, 3 (1973).